OXFORD

Human Molecular Genetics, 2015, 1–11

doi: 10.1093/hmg/ddv109
Advance Access Publication Date: 23 March 2015
Original Article

ORIGINAL ARTICLE

Perinatal *Gjb2* gene transfer rescues hearing in a mouse model of hereditary deafness

Takashi Iizuka[1], Kazusaku Kamiya[1], Satoru Gotoh[2], Yoshinobu Sugitani[2], Masaaki Suzuki[3], Tetsuo Noda[2,4], Osamu Minowa[2,4] and Katsuhisa Ikeda[1,*]

[1]Department of Otorhinolaryngology, Juntendo University Faculty of Medicine, Tokyo 113-8421, Japan, [2]Department of Cell Biology, Japanese Foundation for Cancer Research, Cancer Institute, Tokyo 135-8550, Japan, [3]Department of Otolaryngology, Teikyo University Chiba Medical Center, Ichihara 299-0111, Japan and [4]Team for Advanced Development and Evaluation of Human Disease Models, RIKEN BioResource Center, Tsukuba 305-0074, Japan

*To whom correspondence should be addressed at: Department of Otorhinolaryngology, Juntendo University Faculty of Medicine, 2-1-1 Hongo, Bunkyo-ku, Tokyo 113-8421, Japan. Tel: +81 358021094; Fax: +81 356890547; Email: ike@juntendo.ac.jp

Abstract

Hearing loss is the most widespread sensory disorder, with an incidence of congenital genetic deafness of 1 in 1600 children. For many ethnic populations, the most prevalent form of genetic deafness is caused by recessive mutations in the gene gap junction protein, beta 2, 26 kDa (*GJB2*), which is also known as connexin 26 (*Cx26*). Despite this knowledge, existing treatment strategies do not completely recover speech perception. Here we used a gene delivery system to rescue hearing in a mouse model of *Gjb2* deletion. Mice lacking *Cx26* are characterized by profound deafness from birth and improper development of cochlear cells. Cochlear delivery of *Gjb2* using an adeno-associated virus significantly improved the auditory responses and development of the cochlear structure. Using gene replacement to restore hearing in a new mouse model of *Gjb2*-related deafness may lead to the development of therapies for human hereditary deafness.

Introduction

Severe-to-profound genetic hearing loss affects approximately one in 1600 children (1). Although early management of hearing impairment with hearing aids and cochlear implants often improves speech perception, profoundly deaf children cannot completely acquire the ability to develop spoken language, and thus intelligible speech is severely restricted (2). Gene therapy may become a powerful technology that could fundamentally correct the disease phenotype of genetic deafness. However, gene replacement approaches for animal models of inherited deafness have been extremely limited (3–7).

Currently 160 loci for the monogenic forms of human deafness have been reported, and 60 genes have been identified (see http://hereditaryhearingloss.org/). The most prevalent form of genetic hearing loss in many ethnic populations is due to defects in the gene encoding connexin26 (*GJB2*), which is expressed in the non-sensory cells of the cochlea. The *GJB2* mutations cause between one-third and 50% of prelingual genetic non-syndromic hearing loss, including dominant and recessive mutations (1).

In the inner ear of mice, both a spatially specific approach that targeted the deletion of the *Gjb2* in the cochlear sensory epithelium resulted in the death of different types in the inner ear after onset of hearing (8). On the other hand, a dominant-negative *Gjb2* R75W transgenic mouse created in our laboratories clearly showed incomplete development of the cochlear supporting cells, resulting in profound deafness from birth (9,10). The outer hair cells from the dominant-negative mutation of *Gjb2* showed normal development and maturation (11). Furthermore, three independent lines of conditional Cx26 null mice, which were generated by methods different from those of the previous study, revealed that postnatal development of the organ of Corti was

Received: February 13, 2015. **Revised and Accepted:** March 17, 2015

arrested before the occurrence of cell death in the organ of Corti (12). Thus, *Gjb2* appears to be indispensable in the postnatal development of the organ of Corti and normal hearing. Very recently, we developed a conditional Cx26-deficient mouse with a localized gene deletion in the inner ear under the control of the Protein 0 (P0) promoter. Wild-type mice revealed that both Cx26 and Cx30 were expressed at the cell border forming orderly pentagonal or hexagonal outlines in the whole-mount cochlear tissues. On the other hand, the punctate distribution of Cx30 alone was observed along the cell border in the Cx26-deficient mouse (13).

Gene delivery systems must be non-cytotoxic, and must be able to return to a normal physiological state after treatment (14). We developed a technique for successful transgene expression through the round window membrane in the supporting cells of the neonatal mouse cochlea using adeno-associated viral (AAV) vectors without causing additional damage to the cochlear function (15). Therefore, we investigated the efficiency and specificity of transcriptionally targeted AAV vectors to deliver Cx26 into the cochlea of *Gjb2*-deficient neonatal mice. We demonstrated efficient expression of Cx26 in the non-sensory cells of the organ of Corti. In addition, gene transfer prevented the progression into profound deafness as indicated by the functional assessment of hearing when the treatment was performed during the neonatal stage. The successful restoration of hearing mediated by gene replacement in the genetically created deaf mouse model of *Gjb2* could contribute to the development of clinical applications for human hereditary deafness.

Results

Creation of *Gjb2* conditional knockout mice

Mice lacking *Gjb2* exhibit embryonic lethality because of defective glucose transport across the placenta (16). To circumvent this lethality, we deleted *Gjb2* in a specific spatial pattern by crossing Cx26fl/fl mice with mice expressing Cre recombinase under the control of the P0 promoter (P0-Cre; Fig. 1A). P0 promoter activity was clearly observed at the otic vesicle of the mouse (17). To characterize Cx26 expression in the cochlea, we performed immunohistochemistry. High levels of Cx26 protein were detected in the supporting cells of the organ of Corti, spiral limbus and the lateral wall fibrocytes of littermate controls. However, Cx26 was not detected in the cochlear tissues of Cx26fl/flP0-Cre mice (Fig. 1B). To confirm the expression pattern of P0 in the inner ear lineage, P0-Cre mice were crossed with $R26R^{GFP}$ reporter mice, which contained GFP knocked into the *ROSA26* locus, allowing for the activation of GFP using Cre recombinase, and GFP signals were observed at the otocyst (13,17), which is consistent with the finding that Cx26 ablation disrupted gap junction networks within both epithelial and connective tissues.

The body weight and litter size of Cx26fl/flP0-Cre mice were normal, and the only apparent phenotypic difference exhibited by these mice was deafness. We evaluated the auditory function in Cx26fl/flP0-Cre mice by recording the auditory brainstem response (ABR), which is widely used to objectively determine hearing thresholds. Thresholds for the wave III component of the ABR were measured for click and tone burst stimuli of 8, 12, 16 and 20 kHz in adult Cx26fl/flP0-Cre ($n = 5$) and control ($n = 7$) mice; the evaluated mice were 5–6 weeks old (Fig. 1C). ABR thresholds in Cx26fl/flP0-Cre mice were ~100 dB sound pressure level (SPL) for click stimuli (data not shown) and >90 dB SPL for tone bursts. Control mice exhibited normal values for these thresholds (15–20 dB SPL). At P161, cochleae of Cx26fl/flP0-Cre mice showed normal gross anatomy with no obvious collapse or expansion of the Reissner's membrane. No defects were apparent in the tectorial membrane, stria vascularis or spiral ligament in mice lacking *Gjb2* expression, although a dramatic collapse of the organ of Corti including loss of hair cells and supporting cells was evident (Fig. 1D). Transmission electron microscopy showed collapse of both the tunnel of Corti and Nuel's space and deformities in the shapes of supporting cells, despite the presence of hair cells in the Cx26fl/flP0-Cre mice at P35. In contrast, fine structures of the stria vascularis and the spiral ligament were intact (Fig. 1E).

We then measured the endocochlear potential (EP), which is the resting DC potential in the scala media of the cochlea that is produced by the stria vascularis. These measurements were taken from the basal turn. The average EP value in Cx26fl/flP0-Cre mice was 40.3 ± 15.5 mV ($n = 8$), which was significantly reduced as compared with control mice (80.5 ± 10.7 mV, $n = 6$; $P < 0.01$; Fig. 1F). However, the presence of a residual EP value of ~40 mV cannot completely explain the reduced ABR thresholds that characterized the Cx26fl/flP0-Cre mice. The EP is determined by two K^+ diffusion potentials of the stria vascularis across the electrical barrier (18). The latter is closely related to tight junction proteins around the cochlear duct (19–21). Since the EP depression previously reported in *Gjb2*-deficient mice has been explained by the disruption of the reticular lamina (8), the tight junctions between the hair cells and supporting cells were observed. The fine structure of tight junctions within the organ of Corti was well preserved in the Cx26fl/flP0-Cre mice (Fig. 1G). Thus, the EP defects observed in Cx26fl/flP0-Cre mice may have resulted from insufficient K^+ recycling through the gap junction network rather than through a disruption of the intercellular barrier associated with the cochlear duct.

No correction of hearing by AAV-mediated delivery of *Gjb2* to adult *Gjb2*-deficient mice

To potentially rescue deafness using gene therapy, we generated an AAV vector that drove *Gjb2* expression with the cytomegalovirus promoter. This AAV vector that encoded the Cx26 protein was applied to the perilymph through the round window membrane in adult (P42) Cx26fl/flP0-Cre mice. Eight weeks after treatment, the ABR was measured, and cochlear sections were examined for Cx26 expression. Although the Cx26 gene was transduced moderately in the spiral ligament, the spiral limbus and, weakly, in the organ of Corti, the organ of Corti remained collapsed, and no sensory hair cells were observed. Non-treated cochleae did not show restored Cx26 expression and did not have rescued cochlear morphology (Fig. 2A). Furthermore, no significant change in the ABR threshold was measured in treated or non-treated cochleae (Fig. 2B). Thus, delivery of *Gjb2* to the perilymphatic space of adult Cx26fl/flP0-Cre cochleae failed to improve hearing despite the successful restoration of Cx26 expression in the organ of Corti, the spiral ligament and the spiral limbus. This suggests that the secondary degeneration of hair cells observed in adult Cx26fl/flP0-Cre mice was not arrested or repaired by *Gjb2* gene delivery.

Developmental changes associated with auditory function and cochlear morphology in *Gjb2*-deficient mice

We next compared the developmental course of the ABR thresholds between Cx26fl/flP0-Cre and control mice. In controls, the onset of hearing occurred between P11 and P12, and the ABR thresholds essentially reached adult levels between P18 and

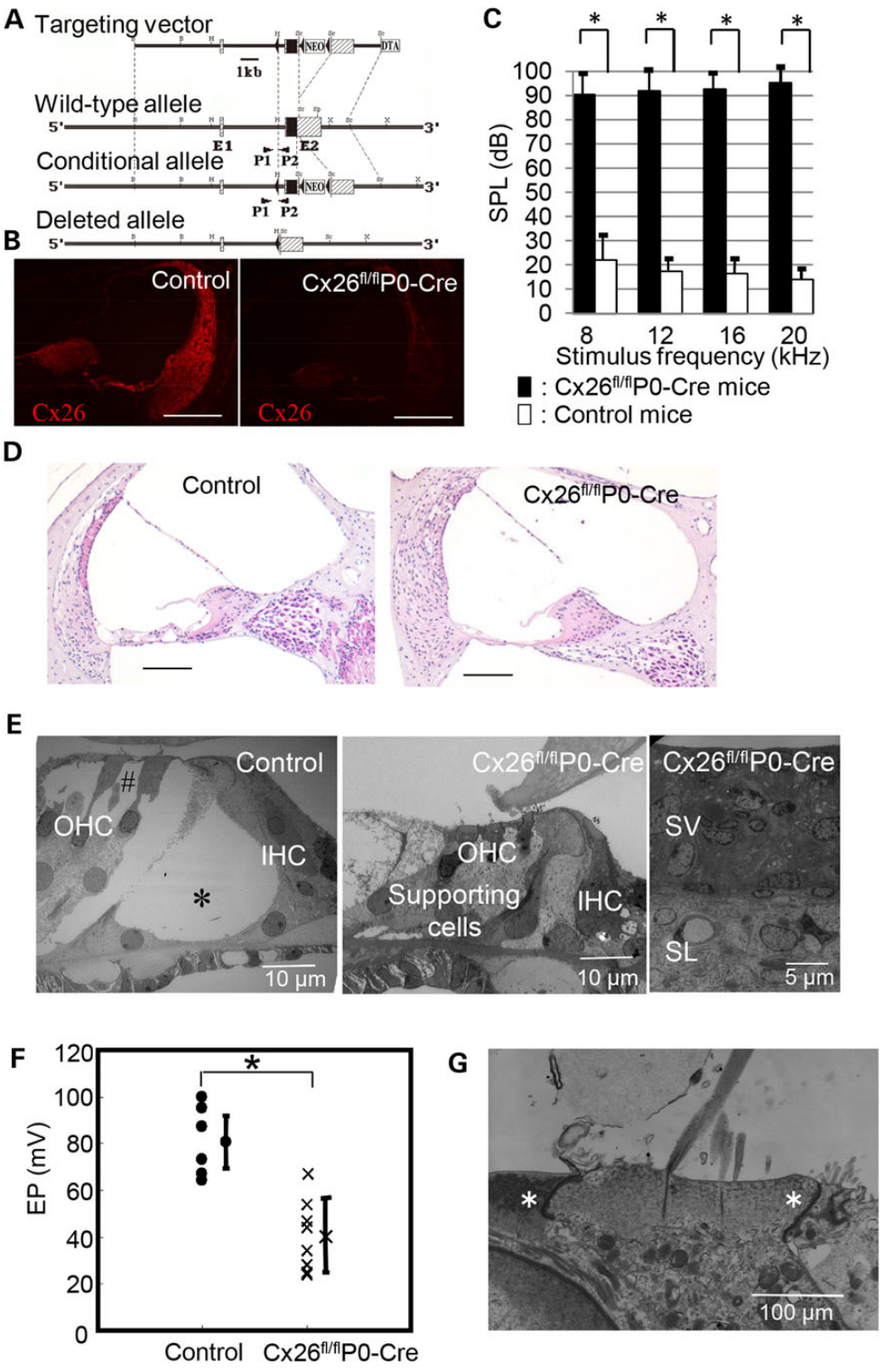

Figure 1. Generation and functional analyses of *Gjb2* conditional knockout mice. (**A**) Structure of the mutated alleles. A *Cx26* conditional knockout allele was generated using a targeting vector containing floxed *Cx26* coding sequences (filled box). LoxP sequences (triangles) and the neomycin resistance gene (NEO; *pMC1-neo*) are shown. B, BamHI; H, HindIII; Sc, SacI; X, XbaI; E1, exon 1; E2, exon 2; DTA, diphtheria toxin A; P1 and P2, PCR primers used for genotyping. (**B**) Cx26 distribution (red) in transverse sections of the cochlear duct of control and $Cx26^{fl/fl}$P0-Cre mice at postnatal day (P)56. (**C**) Average ABR thresholds (dB SPL) to pure tone bursts in control ($n = 7$) and $Cx26^{fl/fl}$P0-Cre ($n = 5$) mice (P35–P42). (**D**) Histological analysis of cochlear structure in control and $Cx26^{fl/fl}$P0-Cre mice (P161). (**E**) Electron micrographs of the organ of Corti in control and $Cx26^{fl/fl}$P0-Cre mice (left two panels). The organ of Corti in the control showed the tunnel of Corti (*) and Nuel's space (#) around the outer hair cells. The stria vascularis and spiral ligament from a $Cx26^{fl/fl}$P0-Cre mouse are shown in the right panel (P35). (**F**) EP in control ($n = 6$) and $Cx26^{fl/fl}$P0-Cre ($n = 8$) mice (P63–P84). *$P < 0.05$ calculated using the Student's *t*-test. (**G**) ZO-1 localization (green) in control and $Cx26^{fl/fl}$P0-Cre mice (top panels). Electron micrograph of tight junctions (*) around hair cells and supporting cells of $Cx26^{fl/fl}$P0-Cre mice (bottom panel). OHC, outer hair cell; IHC, inner hair cell; SV, stria vascularis; SL, spiral ligament; EP, endocochlear potential. Error bars represent the SEM. Scale bars = 100 µm (except for electron micrographs).

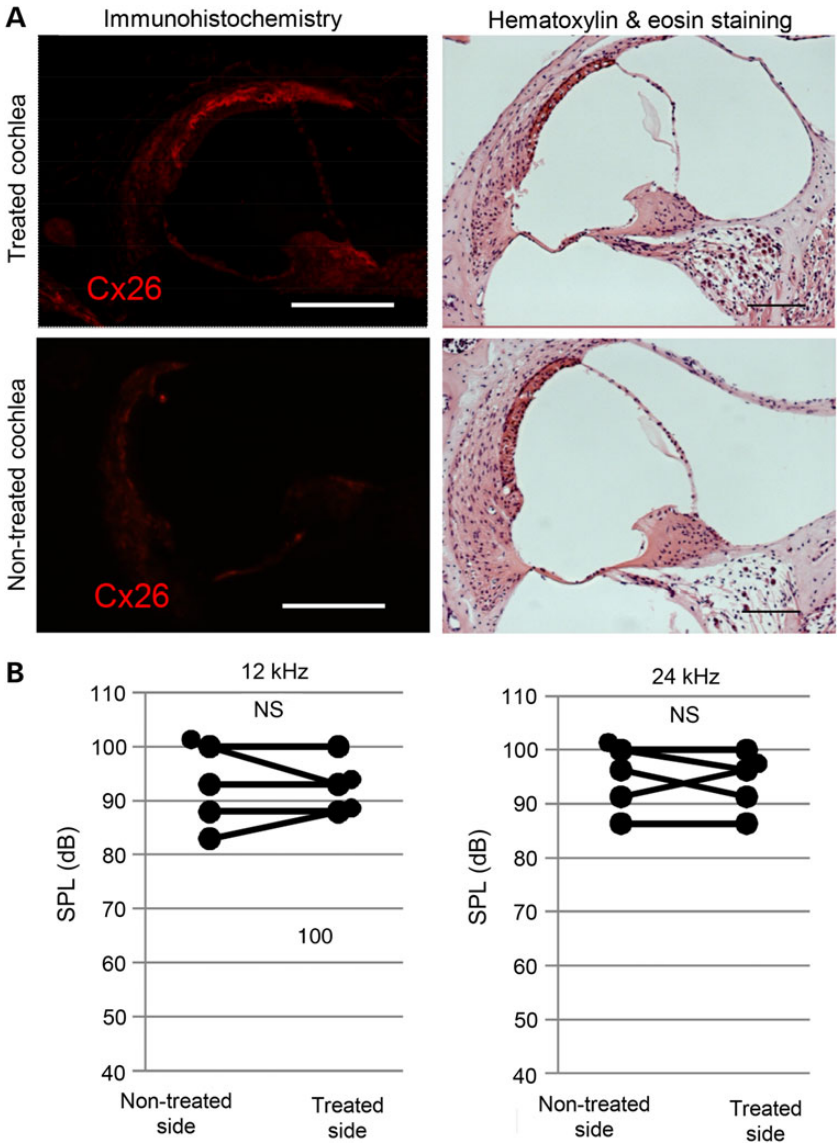

Figure 2. AAV-mediated delivery of *Gjb2* to adult Cx26$^{fl/fl}$P0-Cre mice (P42). (**A**) Cx26 localization (red, left panels) and light micrographs (right panels) of transverse sections of treated and non-treated cochleae from Cx26$^{fl/fl}$P0-Cre mice (P198). (**B**) Average ABR thresholds to pure tone bursts (12 and 24 kHz) in the treated and non-treated side of Cx26$^{fl/fl}$P0-Cre mice (P98; $n = 5$). Significance was calculated using the paired *t*-test. NS, not significant. Scale bars = 100 μm.

P20 (Fig. 3A). For Cx26fl/flP0-Cre mice, however, click stimuli never elicited detectable ABR waveforms, indicating that development of the auditory organ had been disrupted. Histological examination of cochleae from Cx26fl/flP0-Cre mice revealed that the tunnel of Corti, which normally opens by P10, failed to open before the organ of Corti degenerated (Fig. 3B), indicating a developmental defect. In the present mouse model of *Gjb2* deficiency, functional and morphological findings confirmed that *Gjb2* is indispensable during postnatal development of supporting cells in the organ of Corti. In other words, a well-timed transfer of functional *Gjb2* may rescue the postnatal development of the organ of Corti and prevent the secondary degeneration of hair cells.

Successful hearing correction after AAV-mediated delivery of *Gjb2* to neonatal *Gjb2*-deficient mice

We next used a different gene therapy strategy to prevent deafness caused by *Gjb2* deficiency. At P0 (rather than P42), an AAV vector containing wild-type *Gjb2* was introduced into the cochlear perilymph through the round window membrane. We measured the ABR and examined cochlear sections 10–12 weeks post-treatment. A significant improvement in the ABR thresholds was observed (Fig. 4A), together with the successful rescue of Cx26 expression in supporting cells of the organ of Corti, the spiral ligament fibrocytes and the spiral limbus (Fig. 4B). Non-rescued cochleae lacked Cx26 expression in these tissues (Fig. 4B). Fluorescence confocal images in the lateral wall fibrocytes showed that the Cx26 staining was punctate along the plasma membrane (Fig. 4C and D).

Histological examinations revealed proper formation of the tunnel of Corti and preservation of inner and outer hair cells, as well as supporting cells (Fig. 5A). These rescued phenotypes were more apparent at the basal turn than at the apical turn. Morphological differences between turns may have resulted from differential access to the perilymph through the round window membrane. AAV transduction lasted over 6 months (data not shown). Non-rescued cochleae showed unchanged

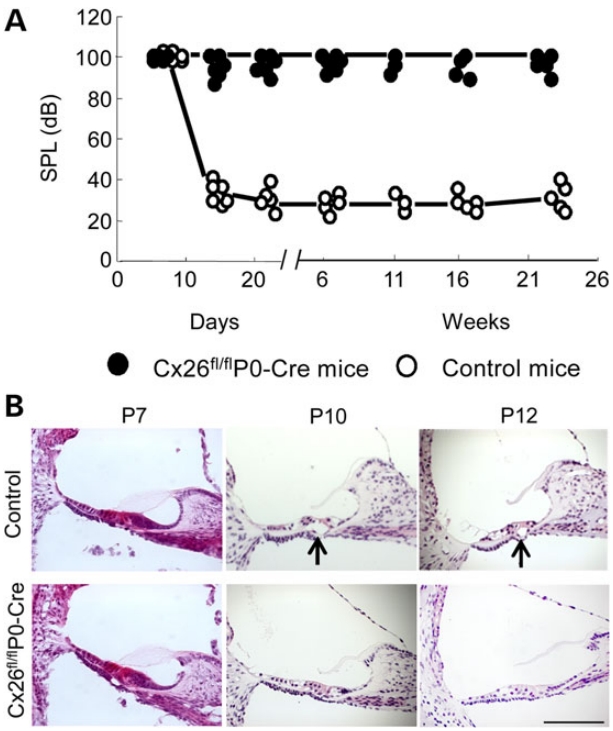

Figure 3. Developmental changes associated with auditory function and cochlear morphology in *Gjb2*-deficient mice. (**A**) Postnatal ABR thresholds to click tones in control and $Cx26^{fl/fl}$P0-Cre mice. (**B**) Transverse sections of the organ of Corti in control and $Cx26^{fl/fl}$P0-Cre mice at P7, P10 and P12. Arrows indicate the tunnel of Corti. Scale bar = 100 μm.

ABR thresholds (Fig. 4A) and collapsed organs of Corti and degenerated hair cells (Fig. 5A). Spiral ganglion neuron degeneration was examined by light microscopy (Fig. 5B). In non-rescued cochleae, both apical and middle turns showed a mild-to-moderate loss of spiral ganglion neurons, whereas a marked reduction in spiral ganglion neurons was observed at the basal turn. Spiral ganglion neurons at the middle and basal turns were apparently better preserved than those in non-rescued cochleae. Quantitative analysis of the height of the pillar cell and the number of spiral ganglion neurons was performed (Fig. 6). The height of the pillar cells of the basal turn in rescued cochleae, which failed to reach full maturation as compared with controls, was significantly increased as compared with that of non-rescued cochleae (Fig. 6A). Quantitative analysis showed that spiral ganglion neuron degeneration progressed from base to apex in *Gjb2*-deficient mice (Fig. 6B). *Gjb2* transfer resulted in a significant increase in the density of neurons at the middle and basal turns. Thus, prevention of both hair cell and spiral ganglion neuron degeneration well explains the preservation of the ABR responses in *Gjb2* transfected cochleae.

Discussion

Using the current mouse model of *Gjb2*-based deafness, we first identified a promising and novel strategy for restoring hearing. Gene therapy failed to rescue hearing in adult *Gjb2*-null mice because secondary hair cell loss was not restored by wild-type *Gjb2*. Performing the gene transfer at early stages of postnatal development, however, i.e. before hair cell degeneration, prevented the onset of deafness. In our laboratory, the gene expression in supporting cells of the neonatal mouse cochlea has been evaluated concerning virus vectors and application routes (15). The extent of adenovirus-GFP transfection was extremely limited in the mesenchymal cells. AAV-directed gene transfer after injection into the scala media through a cochleostomy showed transgene expression in the supporting cells, inner hair cells and lateral wall with resulting hearing loss. On the other hand, gene expression was observed in supporting cells, inner hair cells and lateral wall without hearing loss after the application of AAV into the scala tympani through the round window membrane. Thus, injection of AAV into the scala tympani of the neonatal mouse cochlea was considered to have the potential to efficiently and noninvasively introduce transgenes into the cochlear supporting cells and lateral wall fibrocytes of the neonatal mouse. A successful hearing rescue mediated by AAV-based delivery of a wild-type gene through the round window membrane during early postnatal stages in the present study is well comparable with a previous study to restore hearing in mice carrying a mutation in the vesicular glutamate transporter-3 (*VGLUT3*) (4). However, AAV-driven transfer of *Gjb2* into the scala media of early postnatal conditional *Gjb2* knockout mice did not show significant hearing improvement irrespective of the substantial reduction of both cell death in the organ of Corti and degeneration of spiral ganglion neurons (7). The electrochemical environment in the endolymph is extremely feasible since physiological experiments demonstrated that the injection of volumes >8 nl into the scala media suppressed EP with swollen outer hair cells and shrunken inner hair cells (22). The injection of sodium-based phosphate-buffered solution into potassium-rich endolymph is thought to disturb the mechanotransduction of the hair cells (23). Thus, the subtle change in the cochlear function is likely to be brought about by the endolymphatic application of the vector.

To deliver *Gjb2* to non-sensory cells of the neonatal cochlea, we used an AAV vector that was developed as a stable, efficient and potentially long-term transgene expression system for preserving hearing function in the neonatal cochlea (15) and fetal otocyst (24). The exogenous Cx26 protein in *Gjb2* null mice was expressed in various types of cochlear cells, similar to the expression pattern of GFP protein following AAV-GFP transfection in wild-type mice (15). The same results were also reported in a previous study using another type of *Gjb2*-deficient mice (7). However, in congenital deaf mice lacking *VGLUT3* the expression of VGLUT3 protein was restricted to the targeted cells, namely the inner hair cells (4). Although the underlying mechanism of the difference between *Gjb2* and *VGLUT3* genes is unknown, AAV-*Gjb2* delivery to the *Gjb2* null mice is expected to result in widespread expression in the cochlea. Among available viral vectors, AAV is one of the most promising for use in human clinical trials that involve gene therapy (25). However, the auditory systems of mouse and humans develop quite differently, as the human auditory end organ is almost completely matured by 26–28 weeks of gestation. Therefore, *in uterine* gene therapy must be considered to treat human *GJB2*-related deafness.

Data regarding the Cx function in the cochlea support two hypotheses: (i) the epithelial gap junction network supplies metabolites, nutrients and second messengers that are essential for postnatal development of the organ of Corti (biochemical or metabolic coupling), and (ii) the connective tissue gap junction network recycles K^+ to establish and maintain the ionic and electrical environments of the endolymph after hearing onset (ionic coupling) (9,12,25–31). The development and postnatal maturation of the organ of Corti are affected in a dominant-negative *Gjb2* R75W transgenic mouse (9) and in conditional *Gjb2*-null mice as shown previously (12) and in the present study. Both homomeric (e.g. Cx26 or Cx30) and hybrid (e.g.

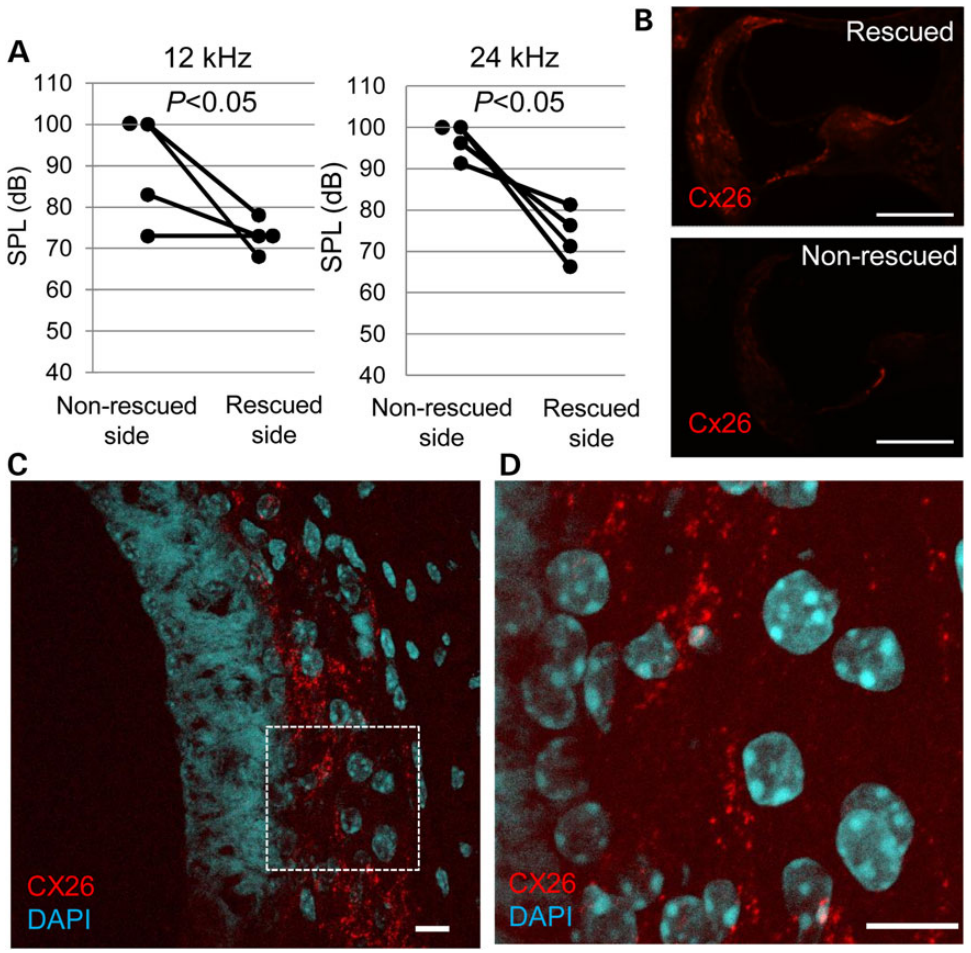

Figure 4. AAV-mediated delivery of *Gjb2* to neonatal (P0) Cx26-deficient mice. (**A**) ABR thresholds to pure tone bursts (12 and 24 kHz) for rescued and non-rescued cochleae of $Cx26^{fl/fl}$P0-Cre mice (P60–P90; $n = 5$). $P < 0.05$ was calculated using the paired *t*-test. (**B**) Cx26 localization (red) after *Gjb2* delivery to $Cx26^{fl/fl}$P0-Cre mice. Scale bars = 100 μm. (**C**) Cx26 distribution (in red) in lateral wall fibrocytes of $Cx26^{f/f}$P0-Cre mice cochlear cryosections at 10 weeks after AAV-Cx26 injection showing the cochlear gap junctions with Cx26. Scale bars: 10 μm. (**D**) A magnified image of region in (C). Nuclei were counterstained with DAPI (blue). Scale bars: 10 μm.

heterotypic and heteromeric Cx26/Cx30) gap junction channels form intercellular networks in non-sensory cells of the cochlea (32,33). Homotypic Cx26 channels, but not homotypic Cx30 channels, are permeable to anion tracers (34). Compared with homomeric channels, hybrid channels relay intercellular Ca^{2+} signals more rapidly (35) and are more permeable to neurobiotin (34). Overexpression of mouse *Gjb2* can rescue hearing loss in *Gjb6/Cx30* null mice (36). In addition, a *Cx30* knockout mouse model that preserved half of the Cx26 expression resulted in normal hearing (37). Thus, biochemical coupling in the cochlea requires hybrid Cx26/Cx30 or homotypic Cx26 gap junctions. Targeted deletion of Cx26 in a mouse model impairs *in vitro* biochemical coupling (7,38). Transducing the cochlear cultures (38) and the scala media (7) with an AAV vector containing Cx26 restores Cx26 expression and rescues biochemical coupling. The rescue of gap junction biochemical coupling may represent the mechanism by which gene transfer restored hearing in our mouse model of Cx26 deficiency. In the present study, gene therapy likely reconstitutes the hybrid Cx26/Cx30 and/or homotypic Cx26 gap junctions in the organ of Corti, as Cx30 was extensively expressed in *Cx26*-deficient mice (13). Restored biochemical or metabolic coupling in the organ of Corti may lead to appropriate postnatal development. To restore hearing, therefore, it may be sufficient to supply a wild-type version of Cx26 only during postnatal development. In contrast, permanent or repeated reconstitution of the K^+ recycling pathway would be required in connective tissue gap junctions. Timed conditional null of Cx26 in mice demonstrated that Cx26 plays essential roles in the maturation process of the organ of Corti prior to the establishment of high K^+ in the endolymph and the onset of hearing (39,40).

The absence of Cx26 or Cx30 is unlikely to disrupt endolymphatic K^+ recycling. The dominant-negative *Gjb2* R75W transgenic mouse is deaf but exhibits a normal EP (9). Normal EP in the dominant-negative R75W mouse can be explained by the fact that homotypic Cx26 channels are permeable to K^+ ions (34,41) and that gap junctions harboring Cx26 mutations associated with hearing loss have no abnormal electrophysiological characteristics, including K^+ permeability (35,36). In Cx30 null mice, the ionic coupling among cochlear supporting cells is indistinguishable from that in wild type (30), and is thought to be easily comparable to that of Cx26 null mice. These findings indicate that the movement of intercellular K^+ can be mediated by gap junction channels composed of Cx30 alone. Lower EP values measured in the current conditional *Gjb2* null mice may reflect reduced K^+ conductance in connective tissues that resulted from a decrease in the total number of gap junction proteins, i.e. the absence of Cx26. The transduction of wild-type Cx26 into cells of the pillar cells is unlikely to be completely sufficient on the basis of the

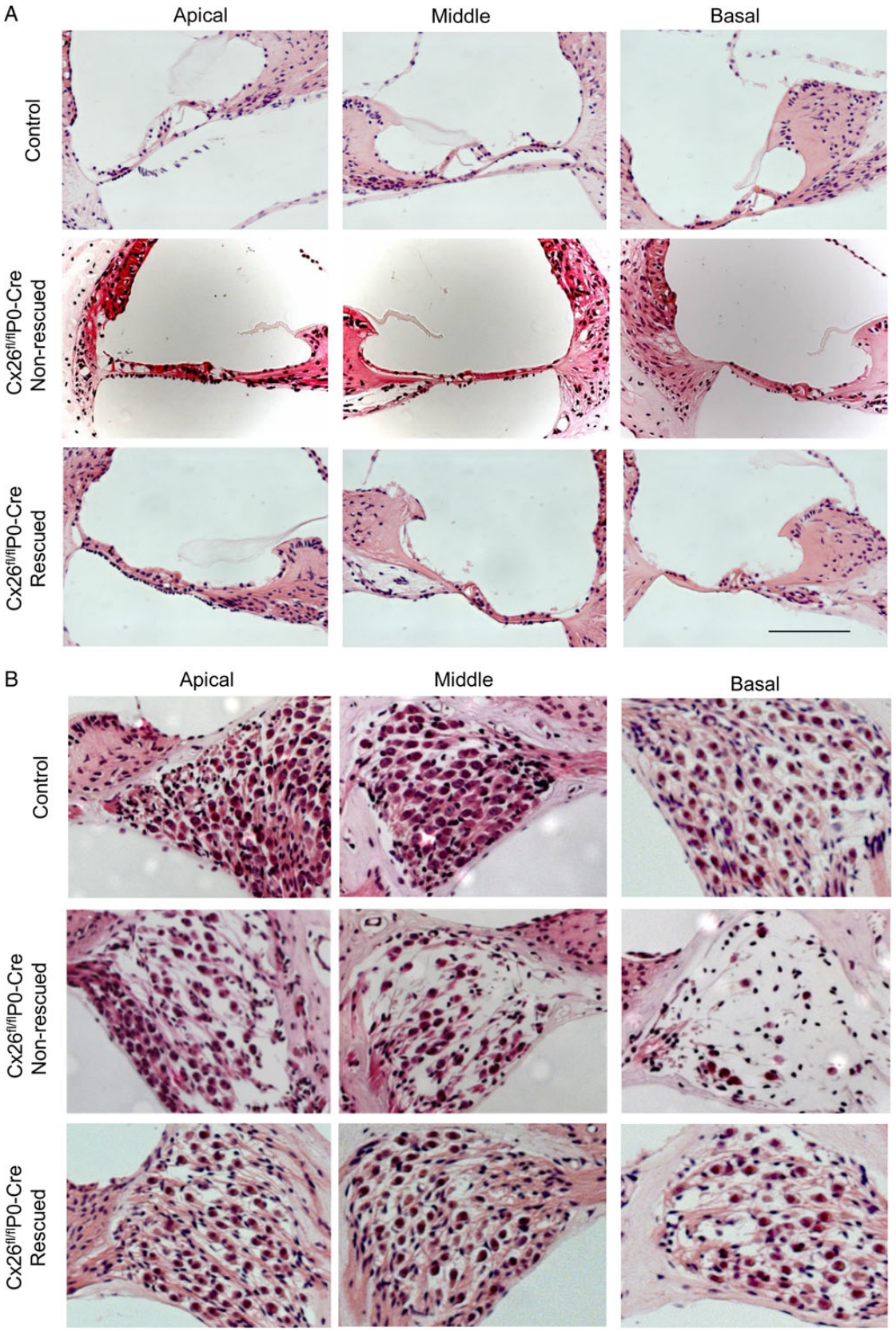

Figure 5. Light micrographs of the organ of Corti (**A**) and the spiral ganglion neurons (**B**) at the apical, middle and basal turns. Images from control mice, non-rescued $Cx26^{fl/fl}$P0-Cre mice and rescued $Cx26^{fl/fl}$P0-Cre mice are shown. Scale bars = 100 μm.

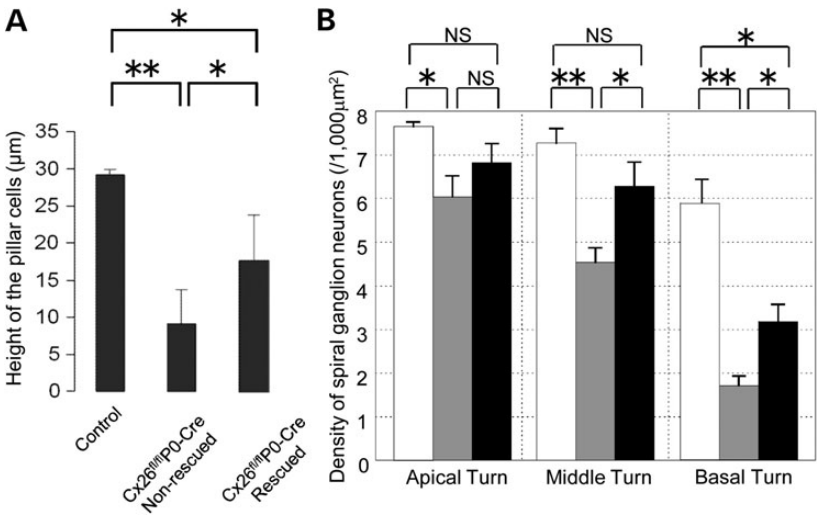

Figure 6. The morphometric analysis derived from Figure 5. (**A**) The height of the pillar cells at the basal turn among control mice and non-rescued and rescued cochleae of $Cx26^{fl/fl}$P0-Cre mice. (**B**) The density of the spiral ganglion neurons among control mice (white columns) and non-rescued (gray columns) and rescued cochleae (black columns) of $Cx26^{fl/fl}$P0-Cre mice. Error bars represent the SEM. Significance (*$P < 0.05$, **$P < 0.01$) was calculated using the Student's *t*-test.

height of the organ of Corti (Fig. 5). The wild-type Cx26 was transduced into type I and IV fibrocytes of the spiral ligament (Fig. 4B), which was consistent with the distribution of native Cx26 (33), suggesting that the EP would likely be partially recovered, although the EP was not measured in rescued cochleae.

Future experiments should focus on improving transduction efficiency to the supporting cells as well as the long-lasting transduction of wild-type Cx26, or replaceable genes such as Cx30 and Cx32 (34,42), in connective tissues.

Using a conditional knockout mouse and gene transfer techniques, we have clarified the molecular mechanisms by which *Gjb2* affects cochlear physiology. The epithelial gap junction network composed of hybrid Cx26/Cx30 channels is required for postnatal development of the organ of Corti and for normal hearing. In contrast, the K^+ recycling pathway, which is mediated by the gap junction network of connective tissues, can be supported by both hybrid and homomeric channels involving Cx26 and/or Cx30. These results will help begin a new era in the comprehensive treatment of hereditary deafness.

Materials and Methods

Generation of mice with a floxed *Cx26* allele

A targeting vector of a floxed *Cx26* allele was constructed using phage DNA clones that included exons 1 and 2 of Cx26 from a genomic library of J1 embryonic stem cells. An ~8.4 kb HindIII–BamHI fragment containing exon 1 and a 2.85 kb 'SacI–SacI' fragment containing the 3′ half of exon 2 (long and short homologous sequences, respectively) were isolated and used to construct the targeting vector. One loxP sequence was introduced at the end of intron 1, and the Neo cassette was introduced between two loxP sequences in exon 2. The diphtheria toxin A chain expression cassette was used as a negative selection marker. The linearized targeting vector was introduced into J1 embryonic stem cells by electroporation, and G418-resistant clones were analyzed by Southern blotting to isolate homologous recombinants as described (43). Recombinant embryonic stem cells were injected into C57/BL6J blastocysts. A mouse strain harboring the floxed Cx26 allele was established by crossing chimeras with C57/BL6J females to produce F1 heterozygotes ($Cx26^{fl/+}$). F2 offspring were generated by crossing two F1 double heterozygotes. Genotyping was performed via PCR amplification using tail lysates as templates and the primers shown in Figure 1A (P1: AAAC TACCGGGAAGCGACACGGGGT; P2: GGTTACGGGGTGCACCAAAG CACAG). No abnormalities were apparent in $Cx26^{fl/fl}$ mice. Otic vesicle-specific Cx26 knockout mice ($Cx26^{fl/fl}$P0-Cre) were generated by breeding $Cx26^{fl/fl}$ mice with P0-Cre mice. All animal work was carried out in accordance with institutional guidelines (see below).

Injection of the AAV-Cx26 viral vector

Animals were anesthetized with an intraperitoneal injection of ketamine (100 mg/kg) and xylazine (10 mg/kg) in all experiments. All experimental protocols were approved by the Institutional Animal Care and Use Committee at Juntendo University School of Medicine and were conducted in accordance with the US National Institutes of Health Guidelines for the Care and Use of Laboratory Animals.

The same protocol was used to treat both the adult and neonatal mice. An AAV serotype 5 vector was generated that used the CMV promoter to drive the expression of mouse Cx26. The coding region from mouse *Gjb2* cDNA (GenBank accession number BC013634.1) was inserted into the *pAAV-IRES-hrGFP* vector (Agilent Technologies, CA, USA). This AAV-Cx26 vector was injected into the perilymph through the round window membrane. Glass capillaries (Drummond Scientific Co., PA, USA) were drawn with a PB-7 pipette puller (Narishige, Tokyo, Japan) to achieve an outer tip diameter of ~10 μm. A polyethylene tube (outer diameter, 1.7 mm; Atom Medical Co., Saitama, Japan) was connected to the glass micropipette. The viral vector with a concentration of 8.6×10^{11} viral particles was injected into the perilymph at a rate of 0.05 μl/min in adult mice and 0.02 μl/min in neonatal mice for 10 min using a syringe connected to a polyethylene tube. To allow the vector to spread throughout the inner ear, the glass micropipette was left in place for 1 min after the injection procedure. The leakage of perilymph was confirmed to be nominal after removing the micropipette. It took ~20 min to complete the surgical procedure. After the surgery, the mice were kept in another cage until they awoke from anesthesia.

Auditory brainstem response

All electrophysiological measurements were performed within a grounded test room that was acoustically and electrically insulated. For the ABR measurement, mice were anesthetized and maintained in a headholder. Stainless steel needle electrodes were placed at the vertex and ventrolateral to the left and right ears. The ABRs were measured using waveform storing and stimulus control with Scope software on the Power Lab system (PowerLab4/25; AD Instruments, Castle Hill, Australia). Electrocardiogram recordings were performed using an extracellular AC Preamplifier (P-55; Astro-Med, Inc., RI, USA). Acoustic stimuli were delivered using a coupler type speaker (ES1spc; Bio Research Center, Nagoya, Japan). Thresholds were determined for click sounds and tone bursts (frequencies of 8, 12, 16, 20 and 24 kHz) from a set of responses at different intensities (5 dB intervals). Electrical signals were averaged over 512 repetitions. Hearing thresholds >95 dB were listed as 100 dB.

Endocochlear potential

For EP measurements, each mouse was artificially ventilated with a respirator through a tracheal cannula after deep anesthesia and muscular relaxation. Rectal temperature was maintained at 37°C, and an electrocardiometer was used to monitor the heart rate. A glass microelectrode filled with 150 mM KCl was inserted into the scala media of the basal turn through the lateral wall of the cochlea as previously reported (44). Output was recorded using a high-impedance dual electrometer.

Light microscopy

Animals were anesthetized and then perfused intracardially with 0.01 M phosphate-buffered saline (PBS; pH 7.2), followed by 4% paraformaldehyde (PFA; pH 7.4) in 0.1 M phosphate buffer (PB; pH 7.4). The mice were decapitated and their cochleae dissected under a microscope. Dissected cochleae were placed in 4% PFA at room temperature overnight. Cochleae were then placed in 0.12 M ethylenediaminetetraacetic acid (EDTA; pH 7.0) in PBS for 1 week for decalcification. Specimens were then dehydrated, embedded in paraffin and sectioned (6 μm). Serial sections were stained with hematoxylin and eosin staining.

Quantitative analyses of spiral ganglion neurons

To evaluate the survival of the spiral ganglion neurons, four animals from each group were used for cell counting. Five cross-sections of hematoxylin and eosin staining randomly selected from each animal were analyzed. The area of the Rosenthal's canal at the basal, middle and apical turns was measured using Image Pro Plus 6.0 software. The number of spiral ganglion neurons per 1000 μm^2 was calculated for each profile.

Transmission electron microscopy

Animals were anesthetized and then perfused intracardially with 0.01 M PBS, followed by 4% PFA and 2% glutaraldehyde (GA) in 0.1 M PB. The cochleae were opened and flushed with buffered 4% PFA and 2% GA and fixed for 2 h at room temperature. The specimens were washed and then post-fixed using 2% OsO_4 in 0.1 M PB for 1.5 h. Specimens were then dehydrated through graded concentrations of ethanol and embedded in Epon. Samples were sectioned (1 μm), stained with uranyl acetate and lead citrate and examined using an electron microscope (H-7100; Hitachi, Tokyo, Japan).

Immunohistochemistry

Mice were anesthetized and then perfused intracardially with PBS, followed by 4% PFA in PB. Cochleae were excised and fixed in 4% PFA for 2 h and then decalcified in 0.12 M EDTA for 7 d at room temperature. For frozen sections, specimens were cryo-protected in 30% sucrose in PBS overnight at 4°C and then embedded in OCT compound, frozen and sectioned (10 μm). For immunofluorescence, sections were incubated with 50% Block Ace (DC Pharma Biomedical, Osaka, Japan) in PBS/0.3% Triton X-100 for 60 min and then incubated overnight at 4°C with rabbit polyclonal antibodies directed against Cx26 and Cx30 (1:200; Zymed laboratories, CA, USA) that were diluted in PBS. Tissue specimens were then rinsed with PBS, incubated with goat anti-rabbit IgG antibodies conjugated with Alexa Fluor 594 (1:500; Molecular Probes, OR, USA) for 60 min and then rinsed with PBS. Specimens were mounted in Vectashield antifade mounting medium (Vector Laboratories, CA, USA). Images were captured using a Zeiss Axioplan2 microscope, an AxioCam HRc CCD camera and AxioVision Rel.4.5 software (Carl Zeiss, Esslingen, Germany). Fluorescence confocal images were obtained with a LSM510-META confocal microscope (Carl Zeiss, Jena, Germany).

Statistical analyses

Error bars represent the SEM. Statistical differences were calculated using the Student's *t*-test or paired *t*-test where indicated. Differences were considered significant for $P < 0.05$.

Authors' Contributions

K.I. and T.N. conceived of and designed the study. S.G., Y.S. and O.M. performed the molecular work. M.S. measured EP. T.I. and K.K. measured ABR and performed the histological experiments. K.I. wrote the paper.

Acknowledgements

We would like to thank H. Yamanaka and S. Ito-Kawashima (Department of Cell Biology, Japanese Foundation for Cancer Research, Cancer Institute) for their technical assistance. We also thank Y. Katori and T. Kudo (Department of Otolaryngology & Head and Neck Surgery, Tohoku University School of Medicine, Sendai); H. Mochizuki (Department of Neurology, Osaka University Graduate School of Medicine, Osaka); T. Nara (Department of Molecular and Cellular Parasitology, Juntendo University Faculty of Medicine, Tokyo); T. Nihira (Department of Neurology, School of Allied Health Sciences, Kitasato University, Sagamihara) and T. Okano, T. Nakagawa and J. Ito (Department of Otolaryngology-Head and Neck Surgery, Kyoto University, Kyoto) for technical advice and valuable discussions.

Conflict of Interest statement. None declared.

Funding

This work was supported in part by grants-in-aid (20390445 and 25293351) to K.I. and by grant-in-aid (12480253) to O.M. from the Ministry of Education, Sports, Science and Culture of Japan, the MEXT-support program for the Strategic Research Foundation at Private Universities, 2011–2013 to K.I. and a research grant from the Ministry of Health, Labor and Welfare of Japan to K.K.

References

1. Petit, C., Levilliers, J. and Hardelin, J.P. (2001) Molecular genetics of hearing loss. *Annu. Rev. Genet.*, **35**, 589–646.
2. Kral, A. and O'Donoghue, G.M. (2010) Profound deafness in childhood. *N. Engl. J. Med.*, **363**, 1438–1450.
3. Maeda, Y., Fukushima, K., Nishizaki, K. and Smith, R.J. (2005) In vitro and in vivo suppression of GJB2 expression by RNA interference. *Hum. Mol. Genet.*, **14**, 1641–1650.
4. Akil, O., Seal, R.P., Burke, K., Wang, C., Alemi, A., During, M., Edwards, R.H. and Lustig, L.R. (2012) Restoration of hearing in the VGLUT3 knockout mouse using virally mediated gene therapy. *Neuron*, **75**, 283–293.
5. Lentz, J.J., Jodelka, F.M., Hinrich, A.J., McCaffrey, K.E., Farris, H.E., Spalitta, M.J., Bazan, N.G., Duelli, D.M., Rigo, F. and Hastings, M.L. (2013) Rescue of hearing and vestibular function by antisense oligonucleotides in a mouse model of human deafness. *Nat. Med.*, **19**, 345–350.
6. Miwa, T., Minoda, R., Ise, M., Yamada, T. and Yumoto, E. (2013) Mouse otocyst transuterine gene transfer restores hearing in mice with connexin 30 deletion-associated hearing loss. *Mol. Ther.*, **21**, 1142–1150.
7. Yu, Q., Wang, Y., Chang, Q., Wang, J., Gong, S., Li, H. and Lin, X. (2014) Virally expressed connexin26 restores gap junction function in the cochlea of conditional Gjb2 knockout mice. *Gene Ther.*, **21**, 71–80.
8. Cohen-Salmon, M., Ott, T., Michel, V., Hardelin, J.P., Perfettini, I., Eybalin, M., Wu, T., Marcus, D.C., Wangemann, P., Willecke, K. and Petit, C. (2002) Targeted ablation of connexin26 in the inner ear epithelial gap junction network causes hearing impairment and cell death. *Curr. Biol.*, **12**, 1106–1111.
9. Kudo, T., Kure, S., Ikeda, K., Xia, A.P., Katori, Y., Suzuki, M., Kojima, K., Ichinohe, A., Suzuki, Y., Aoki, Y., Kobayashi, T. and Matsubara, Y. (2003) Transgenic expression of a dominant-negative connexin26 causes degeneration of the organ of Corti and non-syndromic deafness. *Hum. Mol. Genet.*, **12**, 995–1004.
10. Inoshita, A., Iizuka, T., Okamura, H.O., Minekawa, A., Kojima, K., Furukawa, M., Kusunoki, T. and Ikeda, K. (2008) Postnatal development of the organ of Corti in dominant-negative *Gjb2* transgenic mice. *Neuroscience*, **156**, 1039–1047.
11. Minekawa, A., Abe, T., Inoshita, A., Iizuka, T., Kakehata, S., Narui, Y., Koike, T., Kamiya, K., Okamura, H.O., Shinkawa, H. *et al.* (2009) Cochlear outer hair cells in a dominant-negative connexin26 mutant mouse preserve non-linear capacitance in spite of impaired distortion product otoacoustic emission. *Neuroscience*, **164**, 1312–1319.
12. Wang, Y., Chang, Q., Tang, W., Sun, Y., Zhou, B., Li, H. and Lin, X. (2009) Targeted connexin26 ablation arrests postnatal development of the organ of Corti. *Biochem. Biophys. Res. Commun.*, **385**, 33–37.
13. Kamiya, K., Yum, S.W., Kurebayashi, N., Muraki, M., Ogawa, K., Karasawa, K., Miwa, A., Guo, X., Gotoh, S., Sugitani, Y., Yamanaka, H. *et al.* (2014) Assembly of the cochlear gap junction macromolecular complex requires connexin 26. *J Clin Invest.*, **124**, 1598–1607.
14. Duan, M., Venail, F., Spencer, N. and Mezzina, M. (2004) Treatment of peripheral sensorineural hearing loss: gene therapy. *Gene Ther.*, **11**(Suppl 1), S51–S56.
15. Iizuka, T., Kanzaki, S., Mochizuki, H., Inoshita, A., Narui, Y., Furukawa, M., Kusunoki, T., Saji, M., Ogawa, K. and Ikeda, K. (2008) Noninvasive in vivo delivery of transgene via adeno-associated virus into supporting cells of the neonatal mouse cochlea. *Hum. Gene Ther.*, **19**, 384–390.
16. Gabriel, H.D., Jung, D., Bützler, C., Temme, A., Traub, O., Winterhager, E. and Willecke, K. (1998) Transplacental uptake of glucose is decreased in embryonic lethal connexin26-deficient mice. *J. Cell Biol.*, **140**, 1453–1461.
17. Hasegawa, S., Sato, T., Akazawa, H., Okada, H., Maeno, A., Ito, M., Sugitani, Y., Shibata, H., Miyazaki Ji, J., Katsuki, M. *et al.* (2002) Apoptosis in neural crest cells by functional loss of APC tumor suppressor gene. *Proc. Natl. Acad. Sci. U. S. A.*, **99**, 297–302.
18. Nin, F., Hibino, H., Doi, K., Suzuki, T., Hisa, Y. and Kurachi, Y. (2008) The endocochlear potential depends on two K+ diffusion potentials and an electrical barrier in the stria vascularis of the inner ear. *Proc. Natl. Acad. Sci. U. S. A.*, **105**, 1751–1756.
19. Gow, A., Davies, C., Southwood, C.M., Frolenkov, G., Chrustowski, M., Ng, L., Yamauchi, D., Marcus, D.C. and Kachar, B. (2004) Deafness in Claudin 11-null mice reveals the critical contribution of basal cell tight junctions to stria vascularis function. *J. Neurosci.*, **24**, 7051–7062.
20. Kitajiri, S., Miyamoto, T., Mineharu, A., Sonoda, N., Furuse, K., Hata, M., Sasaki, H., Mori, Y., Kubota, T., Ito, J. *et al.* (2004) Compartmentalization established by claudin-11-based tight junctions in stria vascularis is required for hearing through generation of endocochlear potential. *J. Cell Sci.*, **117**, 5087–5096.
21. Wangemann, P. (2006) Supporting sensory transduction: cochlear fluid homeostasis and the endocochlear potential. *J. Physiol.*, **576**, 11–21.
22. Salt, A.N., Thalmann, R., Marcus, D.C. and Bohne, B.A. (1986) Direct measurement of longitudinal endolymph flow rate in the guinea pig cochlea. *Hear. Res.*, **23**, 141–151.
23. Konishi, T., Kelsey, E. and Singleton, G.T. (1966) Effect of chemical alteration in the endolymph on the cochlear potentials. Acta Otolaryngol. (Stockh.), **62**, 393–404.
24. Bedrosian, J.C., Gratton, M.A., Brigande, J.V., Tang, W., Landau, J. and Bennett, J. (2006) In vivo delivery of recombinant viruses to the fetal murine cochlea: transduction characteristics and long-term effects on auditory function. *Mol. Ther.*, **14**, 328–335.
25. Sacheli, R., Delacroix, L., Vandenackerveken, P., Nguyen, L. and Malgrange, B. (2013) Gene transfer in inner ear cells: a challenging race. *Gene Ther.*, **20**, 237–247.
26. Kikuchi, T., Kimura, R.S., Paul, D.L. and Adams, J.C. (1995) Gap junctions in the rat cochlea: immunohistochemical and ultrastructural analysis. *Anat. Embryol. (Berl)*, **191**, 101–118.
27. Wangemann, P. (2002) K^+ cycling and the endocochlear potential. *Hear. Res.*, **165**, 1–9.
28. Beltramello, M., Piazza, V., Bukauskas, F.F., Pozzan, T. and Mammano, F. (2005) Impaired permeability to Ins(1,4,5)P3 in a mutant connexin underlies recessive hereditary deafness. *Nat. Cell Biol.*, **7**, 63–69.
29. Zhang, Y., Tang, W., Ahmad, S., Sipp, J.A., Chen, P. and Lin, X. (2005) Gap junction-mediated intercellular biochemical coupling in cochlear supporting cells is required for normal cochlear functions. *Proc. Natl. Acad. Sci. U. S. A.*, **102**, 15201–15206.
30. Chang, Q., Tang, W., Ahmad, S., Zhou, B. and Lin, X. (2008) Gap junction mediated intercellular metabolite transfer in the cochlea is compromised in connexin30 null mice. *PLoS One*, **3**, e4088.
31. Majumder, P., Crispino, G., Rodriguez, L., Ciubotaru, C.D., Anselmi, F., Piazza, V., Bortolozzi, M. and Mammano, F. (2010) ATP-mediated cell-cell signaling in the organ of Corti: the role of connexin channels. *Purinergic Signal.*, **6**, 167–187.

32. Ahmad, S., Chen, S., Sun, J. and Lin, X. (2003) Connexins 26 and 30 are co-assembled to form gap junctions in the cochlea of mice. *Biochem. Biophys. Res. Commun.*, **307**, 362–368.
33. Forge, A., Becker, D., Casalotti, S., Edwards, J., Marziano, N. and Nevill, G. (2003) Gap junctions in the inner ear: comparison of distribution patterns in different vertebrates and assessment of connexin composition in mammals. *J. Comp. Neurol.*, **467**, 207–231.
34. Yum, S.W., Zhang, J., Valiunas, V., Kanaporis, G., Brink, P.R., White, T.W. and Scherer, S.S. (2007) Human connexin26 and connexin30 form functional heteromeric and heterotypic channels. *Am. J. Physiol. Cell Physiol.*, **293**, C1032–C1048.
35. Sun, Y., Tang, W., Chang, Q., Wang, Y., Kong, W. and Lin, X. (2009) Connexin30 null and conditional connexin26 null mice display distinct pattern and time course of cellular degeneration in the cochlea. *J. Comp. Neurol.*, **516**, 569–579.
36. Ahmad, S., Tang, W., Chang, Q., Qu, Y., Hibshman, J., Li, Y., Söhl, G., Willecke, K., Chen, P. and Lin, X. (2007) Restoration of connexin26 protein level in the cochlea completely rescues hearing in a mouse model of human connexin30-linked deafness. *Proc. Natl. Acad. Sci. U. S. A.*, **104**, 1337–1341.
37. Boulay, A.C., del Castillo, F.J., Giraudet, F., Hamard, G., Giaume, C., Petit, C., Avan, P. and Cohen-Salmon, M. (2013) Hearing is normal without connexin30. *J. Neurosci.*, **33**, 430–434.
38. Crispino, G., Di Pasquale, G., Scimemi, P., Rodriguez, L., Galindo Ramirez, F., De Siati, R.D., Santarelli, R.M., Arslan, E., Bortolozzi, M., Chiorini, J.A. *et al.* (2011) BAAV mediated GJB2 gene transfer restores gap junction coupling in cochlear organotypic cultures from deaf Cx26Sox10Cre mice. *PLoS One*, **6**, e23279.
39. Chen, S., Sun, Y., Lin, X. and Kong, W. (2014) Down regulated connexin26 at different postnatal stage displayed different types of cellular degeneration and formation of organ of Corti. *Biochem Biophys Res Commun.*, **445**, 71–77.
40. Chang, Q., Tang, W., Kim, Y. and Lin, X. (2015) Timed conditional null of connexin26 in mice reveals temporary requirements of connexin26 in key cochlear developmental events before the onset of hearing. *Neurobiol Dis.*, **73**, 418–427.
41. Manthey, D., Banach, K., Desplantez, T., Lee, C.G., Kozak, C.A., Traub, O., Weingart, R. and Willecke, K. (2001) Intracellular domains of mouse connexin26 and -30 affect diffusional and electrical properties of gap junction channels. *J. Membr. Biol.*, **181**, 137–148.
42. Degen, J., Schütz, M., Dicke, N., Strenzke, N., Jokwitz, M., Moser, T. and Willecke, K. (2011) Connexin32 can restore hearing in connexin26 deficient mice. *Eur. J. Cell Biol.*, **90**, 817–824.
43. Shibata, H., Toyama, K., Shioya, H., Ito, M., Hirota, M., Hasegawa, S., Matsumoto, H., Takano, H., Akiyama, T., Toyoshima, K. *et al.* (1997) Rapid colorectal adenoma formation initiated by conditional targeting of the Apc gene. *Science*, **278**, 120–123.
44. Minowa, O., Ikeda, K., Sugitani, Y., Oshima, T., Nakai, S., Katori, Y., Suzuki, M., Furukawa, M., Kawase, T., Zheng, Y. *et al.* (1999) Altered cochlear fibrocytes in a mouse model of DFN3 nonsyndromic deafness. *Science*, **285**, 1408–1411.